blood

American Society of Hematology
2021 L Street NW, Suite 900,
Washington, DC 20036
Phone: 202-776-0544 | Fax 202-776-0545
editorial@hematology.org

Myeloid Cell-Targeted miR-146a Mimic Inhibits NF-kB-Driven Inflammation and Leukemia Progression *in Vivo*

Tracking no: BLD-2019-002045R1

Yu-Lin Su (City of Hope, United States) Xiuli Wang (City of Hope National Medical Center, United States) Mati Mann (Division of Biology and Biological Engineering, California Institute of Technology, United States) Tomasz Adamus (City of Hope, United States) Dongfang Wang (City of Hope, United States) Dayson Moreira (City of Hope, United States) Zhuoran Zhang (City of Hope, United States) Ching Ouyang (City of Hope National Medical Center, United States) Xin He (city of hope, United States) Bin Zhang (City of Hope, United States) Piotr Swiderski (Beckman Research Institute, United States) Stephen Forman (City of Hope National Medical Center, United States) David Baltimore (California Institute of Technology, United States) Ling Li (City of hope national medical center, United States) Guido Marcucci (Hematologic Malignancies Translational Science, Gehr Family Center for Leukemia Research, City of Hope Medical Center and Beckman Research Institute, United States) Mark Boldin (Beckman Research Institute of the City of Hope, United States) Marcin Kortylewski (Beckman Research Institute at City of Hope, United States)

Abstract:
NF-κB is a key regulator of inflammation and cancer progression, with important role in leukemogenesis. Despite therapeutic potential, targeting NF-κB using pharmacologic inhibitors proved challenging. Here, we describe a myeloid cell-selective NF-κB inhibitor using miR146a mimic oligonucleotide conjugated to a scavenger receptor (SR)/Toll-like receptor 9 (TLR9) agonist (C-miR146a). Unlike an unconjugated miR-146a, C-miR146a was rapidly internalized and delivered to cytoplasm of target myeloid cells and leukemic cells. C-miR146a reduced expression of classic miR-146a targets, *IRAK1* and *TRAF6*, thereby blocking NF-κB activation in target cells. Intravenous injections of C-miR146a mimic to *miR-146*-deficient mice prevented excessive NF-κB activation in myeloid cells, thereby alleviating myeloproliferation and mice hypersensitivity to bacterial challenge. Importantly, C-miR146a showed efficacy in dampening severe inflammation in clinically relevant models of chimeric antigen receptor (CAR) T-cell-induced cytokine release syndrome (CRS). Systemic administration of C-miR146a oligonucleotide alleviated human monocyte-dependent release of IL-1 and IL-6 in xenotransplanted B-cell lymphoma model without affecting CD19-specific CAR T-cell antitumor activity. Beyond anti-inflammatory functions, miR146a is a known tumor suppressor commonly deleted or expressed at reduced levels in human myeloid leukemia. Using TCGA AML dataset, we found inverse correlation of miR-146 levels with NF-κB-related genes and with patients' survival. Correspondingly, C-miR146a induced cytotoxic effects in human MDSL, HL-60 and MV4-11 leukemia cells *in vitro.* The repeated intravenous administration of C-miR146a inhibited expression of NF-κB target genes and thereby thwarted progression of disseminated HL-60 leukemia. Our results demonstrate potential of using myeloid cell-targeted miR146a mimics for treatment of inflammatory and myeloproliferative disorders.

Conflict of interest: COI declared - see note

COI notes: M.K., P.S., G.M. have a patent on C-miRNA conjugates and uses thereof compositions for the treatment of cancers and other diseases. No potential conflicts of interest were disclosed by the other authors.

Preprint server: No;

Author contributions and disclosures: Study design: Y.-L.S., M.K. Data acquisition: Y.-L.S., X.W., M.M., T.A., D.M., Z.Z., D.W., P.S., M.K. Data analysis and interpretation: Y.-L.S., M.M., T.A., D.M., D.W., C.O. Administrative, technical, or material support: Y.-L.S., X.W., X.H., B.Z., P.S., S.F., D.B., L.L., G.M., M.B., M.K. Manuscript writing: Y.-L.S., M.K.

Non-author contributions and disclosures: No;

Agreement to Share Publication-Related Data and Data Sharing Statement: Please email all requests to the corresponding author.

Clinical trial registration information (if any):

Myeloid Cell-Targeted miR-146a Mimic Inhibits NF-κB-Driven Inflammation and Leukemia Progression *in Vivo*

Yu-Lin Su[1], Xiuli Wang[2], Mati Mann[3], Tomasz Adamus[1], Dongfang Wang[1], Dayson Moreira[1], Zhuoran Zhang[1], Ching Ouyang[4.5], Xin He[6], Bin Zhang,[6] Piotr Swiderski[7], Stephen Forman[2], David Baltimore[3], Ling Li[6], Guido Marcucci[2, 6], Mark P. Boldin[8], and Marcin Kortylewski[1, 9, *]

[1]*Department of Immuno-Oncology; Beckman Research Institute at City of Hope Comprehensive Cancer Center, Duarte, CA, USA*

[2]*Department of Hematology and Hematopoietic Cell Transplantation; City of Hope Comprehensive Cancer Center, Duarte, CA, USA*

[3]*Division of Biology and Biological Engineering, California Institute of Technology, Pasadena, CA, USA*

[4]*Center for Informatics, City of Hope National Medical Center, Duarte, CA, USA*

[5]*Department of Computational and Quantitative Medicine, Beckman Research Institute of the City of Hope, Duarte, CA, USA*

[6]*Department of Hematologic Malignancies Translational Science; Gehr Family Leukemia Center at City of Hope Comprehensive Cancer Center, Duarte, CA, USA*

[7]*DNA/RNA Synthesis Core Laboratory; Beckman Research Institute at City of Hope Comprehensive Cancer Center, Duarte, CA, USA*

[8]*Department of Molecular and Cellular Biology; Beckman Research Institute at City of Hope Comprehensive Cancer Center, Duarte, CA, USA*

[9]*Center for Gene Therapy; Beckman Research Institute at City of Hope Comprehensive Cancer Center, Duarte, CA, USA*

*Correspondence should be addressed to:

Marcin Kortylewski, Ph.D.; e-mail: mkortylewski@coh.org

Running Title: Myeloid cell-targeted miR146a for NF-κB inhibition

Total word count: 3987 (Abstract: 245)

Total number of figures and tables: 6

References: 50

KEY POINTS

■ Synthetic C-miR146a mimic inhibits inflammatory and tumorigenic NF-κB activity in macrophages and myeloid leukemia *in vitro* and *in vivo*.

■ C-miR146a alleviates monocyte-mediated cytokine storm without affecting CD19-specific CAR T-cell activity against B-cell lymphoma.

ABSTRACT

NF-κB is a key regulator of inflammation and cancer progression, with important role in leukemogenesis. Despite therapeutic potential, targeting NF-κB using pharmacologic inhibitors proved challenging. Here, we describe a myeloid cell-selective NF-κB inhibitor using miR146a mimic oligonucleotide conjugated to a scavenger receptor (SR)/Toll-like receptor 9 (TLR9) agonist (C-miR146a). Unlike an unconjugated miR-146a, C-miR146a was rapidly internalized and delivered to cytoplasm of target myeloid cells and leukemic cells. C-miR146a reduced expression of classic miR-146a targets, *IRAK1* and *TRAF6*, thereby blocking NF-κB activation in target cells. Intravenous injections of C-miR146a mimic to *miR-146*-deficient mice prevented excessive NF-κB activation in myeloid cells, thereby alleviating myeloproliferation and mice hypersensitivity to bacterial challenge. Importantly, C-miR146a showed efficacy in dampening severe inflammation in clinically relevant models of chimeric antigen receptor (CAR) T-cell-induced cytokine release syndrome (CRS). Systemic administration of C-miR146a oligonucleotide alleviated human monocyte-dependent release of IL-1 and IL-6 in xenotransplanted B-cell lymphoma model without affecting CD19-specific CAR T-cell antitumor activity. Beyond anti-inflammatory functions, miR146a is a known tumor suppressor commonly deleted or expressed at reduced levels in human myeloid leukemia. Using TCGA AML dataset, we found inverse correlation of miR-146 levels with NF-κB-related genes and with patients' survival. Correspondingly, C-miR146a induced cytotoxic effects in human MDSL, HL-60 and MV4-11 leukemia cells *in vitro.* The repeated intravenous administration of C-miR146a inhibited expression of NF-κB target genes and thereby thwarted progression of disseminated HL-60 leukemia. Our results demonstrate potential of using myeloid cell-targeted miR146a mimics for treatment of inflammatory and myeloproliferative disorders.

INTRODUCTION

MicroRNAs (miRNAs) are small non-coding RNAs that control expression of a broad set of target genes based on sequence complementarity. By binding to the target mRNA's 3' untranslated regions (3'UTR), miRNAs regulate gene expression and enable control of multiple gene targets within the same or distinct signaling pathways.[1,2] Many miRNAs are dysregulated in cancer, cardiovascular and autoimmune diseases.[3] Genomic mutations, deletion, or changes in the key enzymes in miRNA biogenesis may all lead to alterations in miRNA levels.[4,5] Genome-wide miRNA screening of leukemia-associated loci identified miR146a as major mediator of the chromosome-5q deletion myelodysplastic syndrome, del(5q) MDS, and acute myeloid leukemia (AML).[6-8] The reduced miR-146a expression contributes to the development of del(5q) MDS and progression to AML through IRAK1- and TRAF6-dependent activation of NF-κB.[9,10] In non-malignant myeloid cells, such as monocytes, decreased miR-146a levels result in expression of IL-6 and other proinflammatory mediators implicated in the pathogenesis of autoimmune diseases and cancers.[11-13] The miR-146a dysregulation and IL-6 elevation in hematopoietic stem/progenitor and myeloid cells is also associated with many autoinflammatory disease such as rheumatoid arthritis, systemic lupus erythematosus, type II diabetes, Sjogren's syndrome and endotoxemia-related cytokine storm.[14] While the role of miR146a is yet unclear, the NF-κB-mediated release of IL-6 from monocyte was also shown responsible for cytokine release syndrome (CRS), a serious adverse effect of CAR T-cell therapies.[12,15] Due to lack of pharmacologic NF-κB inhibitors, synthetic miRNA146a mimics are an attractive opportunity for immunomodulation or elimination of tumorigenic signaling. However, the effective delivery of miRNA therapeutics is challenging, complicated by safety concerns and potential off-target effects.[2,16] Several types of miRNA delivery vehicles, including liposomes, lipid nanoparticles, dendrimers or hydrogels were tested before.[17-19] Only a few of synthetic miRNA mimics, including anti-fibrotic and TGFβ-targeting miR-29/Remlarsen, progressed to initial clinical testing.[19] Here, we describe an original approach for the targeted delivery of chemically-modified miR146a mimic to myeloid cells and verify miR146a mimic activity in models of inflammatory and myeloproliferative diseases.

METHODS

Mice and *in vivo* studies

All animal experiments were following institutional guidance and approved protocols from the Institutional Animal Care and Use Committee. C57BL/6, BALB/c mice 6-8 weeks of age were purchased from the National Cancer Institute, female C.B-*Igh*-1b/GbmsTac-*Prkdc*^{scid}-*Lyst*^{bg}N7 (SCID-Beige) mice were from Taconic, *NOD/SCID/IL-2RgKO* (NSG) and NSG Tg(*IL3,CSF2,KITLG*)*1Eav/MloySzJ* (SGM3) mice were from Jackson Laboratory. *miR-146a*$^{-/-}$ and *LyzM-Cre/miR-146a*$^{fl/fl}$ mice[9,20] were bred and housed in Laboratory Animal Resources facility at Caltech.

C-miR146a synthesis

The C-miR146a conjugates were synthesized in the DNA/RNA Synthesis Core (COH) by linking CpG-D19 to miR-146a passenger strands as described.[21] These were hybridized with complementary guide strands of mature miR-146a creating chimeric C-miR146a mimic. The single stranded sequences are listed below (x = C3-unit; asterisks = phosphorothioation; underline = 2'O-methylation):

C-miR146a passenger:

5' G*G*TGCATCGATGCAGG*G*G*G*G-xxxxx-CCCAUGGAAUUCAGUUCUCAAA 3'.

miR146a guide:

5' UGAGAACUGAAUUCCAUGGGUU 3'.

C-scrRNA passenger:

5' G*G*TGCATCGATGCAGG*G*G*G*G -xxxxx-AUUUAGCCUUAAUACACGCCAA 3'

scrRNA guide:

5' GGCGUGUAUUAAGGCUAAAUCU 3'

For internalization studies, the miR146a guide strand was labeled on 3' end using Cy3 fluorochrome.

RNA-binding protein immunoprecipitation

The RNA-binding protein immunoprecipitation/RIP was performed using Magna RIP kit (Millipore) according to manufacturer's instructions. Details described in the Supplemental Methods.

***In vivo* bio-distribution**

miR-146a$^{-/-}$ mice or syngeneic *Cbfb/Myh11/Mpl* mouse leukemia-bearing C57BL/6 mice were injected retro-orbitally with 2.5-20mg/kg C-miR146a, C-miR146a^{Cy3} or miR146a^{Cy3} as described before.[22] At indicated times, mice were euthanized to collect organs for flow cytometry, qPCR or Western blot analysis. EasySep PE-positive selection kits (Stemcell) were used for cell subset enrichment.

***Listeria monocytogenes* studies**

10^5 c.f.u. of *Listeria monocytogenes* (strain-10,403/serotype-1) was injected to each WT C57BL/6 or *LyzM-Cre/miR-146a*$^{fl/fl}$ mice using retro-orbital injections. Mice were treated every day using 5mg/kg C-miR146a or C-scrRNA (negative control) for three days before and three days after infection. The mice were euthanized, various organs were collected for further analysis.

Cytokine release syndrome models

For *in vitro* studies, mock or CD19 CAR T cells from four donors were cultured with target Nalm6 leukemia with or without CD14+ monocytes from same donor. Healthy donors' PBMCs were collected according to Declaration of Helsinki. The co-cultured cells were treated with C-miR146a or C-scrRNA (500nM) for 2 days. After 48h, supernatants were collected and IL-1 and IL-6 levels were analyzed using ELISA (Thermo Fisher). *In vivo* CRS studies used female SCID-Beige mice

injected using 3×10^6 Raji$^{GFP/Luc}$ cells, following with intraperitoneal injections of C-miR146a (5mg/kg) or PBS daily for three days before transfer of 12.5×10^6 mock-transfected or CD19-specific CAR-T-cells described before.[15,23,24]

Human AML xenotransplants

NSG-SGM3 mice were injected intravenously with 2×10^6 of HL-60^{LUC} cells and tumor progression was monitored using BLI/AmiX (Spectral Instruments). Mice were injected retro-orbitally with 10mg/kg of C-miR146a or C-scrRNA every other day. Total RNA was isolated from bone marrow cells and analyzed using RT^2 Profiler PCR Arrays (Qiagen).

Gene expression analysis

The overall survival analysis was conducted using R package *survival* (vs.2.44.1.1). Log-rank statistics were applied to identify the optimal cut-point for transforming the continuous variable of gene expression into categorical high and low expression groups in a survfit model, using the *cutp* function of the R package *survMisc* (vs.0.5.5).

Statistics

Unpaired *t* test was used to calculate two-tailed *P* value to estimate statistical significance between two treatment groups. One- or two-way ANOVA plus Bonfeerroni post-test assessed differences between multiple groups or in tumor growth kinetics, respectively. Statistically significant *P* values were indicated in figures compared to untreated or PBS groups. Data analyzed using Prism software v.7 (GraphPad).

RESULTS

Targeted delivery of functional miR-146a mimic into myeloid cells and B-cells

To overcome challenges in the efficient and cell-selective delivery of miR-146a, we modified the scavenger receptor (SR)/Toll-like receptor 9 (TLR9)-targeting platform originally developed for transfer of 25/27-mer Dicer-substrate siRNA.[21] The double-stranded miR-146a was conjugated through 5' end of the passenger strand to the 3' end of a single-stranded, partly phosphorothioated oligodeoxynucleotide (CpG ODN) using a synthetic carbon linker. The specific type-A CpG ODN sequence of the conjugate was selected for monocytes/myeloid cell specificity[25] and poor ability to activate NF-κB and its downstream IL-6 and IL-10 targets.[26] To ensure the maximum activity and target specificity, the miR-146a was chemically modified for nuclease resistance by a 2'O-methyl-modification in the 3' end of passenger strand (Figure 1A). This design significantly improved serum stability of the C-miR-146a conjugate without impacting activity. Compared to miR-146a ($T_{1/2}$~1h), the conjugated C-miR146a had 34h half-life in human serum (Figure 1B and Supplemental Fig.S1). The C-miR146a^{Cy3} was rapidly internalized by primary human immune cells and mouse RAW264.7 macrophages (Figure 1C) or splenocytes (Supplemental Fig.S2) within 1h of incubation, without any transfection reagents. Compared to the unconjugated miR146a^{Cy3}, C-miR146a^{Cy3} was also efficiently taken up by human MDSL or HL60 myeloid leukemia cells, Raji Burkitt's lymphoma cells but not human T-cell leukemia TAIL7 cells (Figure 1C). The uptake of C-miR146a depended on the scavenger receptor A- and clathrin-mediated endocytosis, as verified using internalization inhibitors, specifically dextran sulfate, fucoidan and cadaverine (Supplemental Fig.S3). TLR9 commonly expressed by myeloid and B-cell malignancies, including tested myeloid leukemia and B-cell lymphoma cells (Supplemental Fig.S 4).[26] Confocal microscopy showed that C-miR146a localized to the cytosol of target cells within 1h, while miR-146a alone was undetectable (Figure 1D). To inhibit target mRNAs, the miRNA guide strand must bind Argonaute-2 (Ago2) protein within the RNA-induced silencing complex (RISC). To assess whether the guide strand of C-miR146a was successfully loaded onto the RISC, we performed RNA-binding protein immunoprecipitation (RIP) using Ago2-specific antibodies (Figure 1E). In fact, the level of Ago2-bound miR-146a guide strand increased several fold in mouse RAW264.7 macrophages incubated with the C-miR146a but not with miR-146a. This effect was even more prominent in primary mouse splenocytes derived from

miR-146a$^{-/-}$ mice (Figure 1E). These results indicated that the C-miR146a allows for the delivery of functional miR-146a to human and mouse myeloid target cells.

C-miR146a mimic targets upstream regulators of NF-κB signaling

MiR-146a targets IRAK1 and TRAF6, the critical upstream regulators of NF-κB signaling.[10] We used 3'-UTR-luciferase reporter assays to verify whether C-miR146a can alter *IRAK1* and *TRAF6* expression. As shown in Figure 2A, C-miR146a conjugate reduced *IRAK1* and *TRAF6* 3'-UTR-luciferase reporter activities in sequence-specific manner as verified by mutating 3'-UTR sequences (Figure 2A). Neither miR-146a alone nor negative control scrambled RNA (C-scrRNA) affected these 3'-UTR-luciferase reporters. Moreover, C-miR146a, but not the control oligonucleotides, reduced IRAK1 and TRAF6 protein levels in mouse RAW264.7 macrophages but only IRAK1 in human MDSL cells (Figure 2B). Lack of TRAF6 inhibition by C-miR146a is likely related to a mutation in one of miR-146a binding sites in *TRAF6* 3'UTR in human MDSL cells (Supplemental Fig.S5). Activated NF-κB translocates to the nucleus, thus we examined the effect of C-miR146a on the localization of NF-κB in LPS-treated RAW264.7 cells expressing NF-κB/p65-eGFP fusion protein.[27] Confocal microscopy confirmed that C-miR146a, but not C-scrRNA, efficiently blocked the nuclear translocation of NF-κB (Figure 2C). Correspondingly, the C-miR146a reduced the NF-κB DNA-binding activity in nuclear extracts from RAW264.7 and MDSL cells as measured using gelshift assays (Figure 2D). These C-miR146a effects reduced LPS-induced transcriptional NF-κB activity in RAWBlue macrophages (Figure. 2E) and secretion of IL-6 by parental RAW264.7 cells (Figure 2F).

For an additional verification that the observed effects sequence-specific, we used analogical approach to deliver miR146a-targeting antisense oligonucleotide, C-anti-miR146a (Supplemental Fig.S6A).[28] C-anti-miR146a showed similar cell-selectivity as C-miR146a mimic (Supplemental Fig.S6B) but opposite biological activity. C-anti-miR146a knocked-down *miR-146a* in mouse splenocytes and myeloid cells (Supplemental Fig.S6C), thereby upregulating *IRAK1* and *TRAF6* 3'UTR activities (Supplemental Fig.S6DE), NF-κB DNA-binding (Figure 2D) and nuclear translocation (Supplemental Fig.S6F). Taken together, the

flexibility of our strategy permits positive or negative regulation of NF-κB activity using SR/TLR9-mediated miR-146a mimic or antisense delivery, respectively.

Systemic C-miR146a mimic delivery restored control over IRAK1 and TRAF6 in *miR-146a*-deficient myeloid cells *in vivo*

Treatment of NF-κB-related disorders requires efficient delivery of miR146a mimic to target myeloid cells in various organs. To directly quantify the dose- and time-dependent biodistribution of C-miR146a mimic in the absence of endogenous miR146a, we used the real-time qPCR to detect miR-146a guide-strand in various organs of *miR-146a*-deficient mice.[9] Our initial pharmacokinetic analysis found that C-miR146a reaches maximum plasma level ~30 min after intravenous injection, with 144 min circulatory half-life (Supplemental Fig.S7). Consistently, we found dose-dependent accumulation of miR-146a guide-strand in bone-marrow, spleens and lymph nodes of *miR-146a*$^{-/-}$ mice following IV-injection of C-miR146a (Figure 3A). In 2.5-20mg/kg dose-range, C-miR146a delivered miR-146a-5p guide-strand preferentially to CD11b^{+} myeloid cells from bone-marrow (Figure 3B). For more precise identification of target cells, we injected IV fluorescently-labeled C-miR146a^{Cy3} or miR146a^{Cy3} (5mg/kg) into AML-bearing mice and analyzed their cellular uptake after 3h using flow cytometry. C-miR146a^{Cy3} was internalized by ~30-50% of various myeloid cells and leukemic cells, ~20% of long-term HSCs, minimally by B and NK cells but not by T cells (Figure 3C). As expected, cellular uptake of miR146a^{Cy3} alone was negligible. Next, we compared the miR-146a levels in oligonucleotide-treated *miR-146a*$^{-/-}$ mice to the untreated wild-type (WT) mice to quantify the relative miR-146a restoration in specific immune cell populations. As shown in the Figure 3D, the single injection of 5mg/kg C-miR146a to *miR-146a*$^{-/-}$ mice replaced ~61% and ~53% of WT miR-146a levels in bone marrows and spleens, respectively. MiR-146a was restored to ~47%, ~28% and ~5% of the WT levels, in splenic CD11b^{+} myeloid cells, CD19^{+} B-cells and CD3^{+} T-cells, respectively (Figure 3E), confirming preferential myeloid cell-targeting. Finally, we have tested whether partial restoration of miR-146a will have sufficient biological activity to inhibit target IRAK1 and TRAF6 proteins. In fact, within 12-24h after a single IV injection of C-miR146a (5mg/kg), both IRAK1 and TRAF6 were reduced close to the WT levels, returning

to the baseline after 2-3 days (Figure 3F). These results indicate that systemic delivery of C-miR146a using relatively low dosing can transiently restore levels and full biological activity of miR-146a in target myeloid cells *in vivo*.

C-miR146a abrogates myeloproliferation and exaggerated inflammatory responses in *miR146a*-deficient mice

Expansion of myeloid cells is one of the critical phenotypic features of the *miR-146a*-deficient mice.[29] Compared to WT mice, bone marrow-derived macrophages (BMDMs) from *miR-146a*-deficient mice show enhanced proliferation accompanied by elevated expression of colony–stimulating factor–1 receptor (CSF1R).[30] Therefore, we examined whether delivery of C-miR146a to *miR-146a*$^{-/-}$ BMDMs prevents the aberrant myeloproliferation. In fact, the C-miR146a but not C-scrRNA treatment reduced proliferative rate of *miR-146a*$^{-/-}$ BMDMs close to the WT BMDMs (Figure 4A). Together with the reduced proliferation, the elevated cell surface levels of CSF1R on *miR-146a*$^{-/-}$ BMDMs were reduced by C-miR146a to baseline WT levels (Figure 4B). Consistently, repeated two-week C-miR146a treatment of aged *miR-146a*$^{-/-}$ mice reduced the expansion of immature CD11b^{+}Gr1^{+} myeloid cells, together with their proliferation and CSF1R expression on macrophages (Figure 4C-E).

Next, we examined whether miR146a mimic delivery can attenuate the exaggerated inflammatory response to a systemic bacterial endotoxin challenge resulting from the miR-146a ablation.[30] Age- and gender-matched WT and *miR-146a*$^{-/-}$ mice were injected with a sub-lethal dose of LPS, and the plasma levels of pro-inflammatory cytokines, IL-6 and TNF-α, were measured using ELISA. As expected, LPS induced a higher and more prolonged cytokine response in *miR-146a*$^{-/-}$ mice than in WT mice, peaking at 2-6h before returning to baseline at 24h. In contrast, C-miR146a treatment reduced IL-6 and TNF-α upregulation in *miR-146a*$^{-/-}$ mice at both 2 and 6h compared to C-scrRNA control treatment (Figure. 4F). The effect of C-miR146a on the inflammatory cytokine secretion in WT mice was minimal, indicating the adequate negative control of cytokine production by the endogenous miR146a. Following on these results, we used mice with the myeloid cell-specific miR-146a ablation (*LyzM-Cre/miR-146a*$^{fl/fl}$) to assess the effect of miR-146a

restoration on the IL-6-controlled response to a bacterial infection with *Listeria monocytogenes*.[20,31,32] Both WT and *miR-146a*$^{fl/fl}$ mice were injected daily with C-miR146a or control C-scrRNA (5mg/kg) starting 3 days before the sublethal infection with *L. monocytogenes*. The C-miR146a treatment interfered with the bacterial clearance in *miR-146a*-deficient and WT mice increasing bacterial burden in liver and spleen (Figure 4G and Supplemental Fig.S8A). The reduced bacterial load in control-treated *miR-146a*$^{fl/fl}$ mice correlated with weight loss (Figure 4H) and elevated plasma levels of IL-6 (Figure 4I). All these effects of miR146a-deletion were completely alleviated by C-miR146a treatment. Finally, miR-146a restoration decreased the expansion of CD11b^{+} myeloid cells, including Gr1^{+} granulocytes, in blood and spleen of control *miR-146a*$^{fl/fl}$ mice (Figure 4J and Supplemental Fig.S8B). Taken together, our results indicate that myeloid cell-targeted miR-146a restoration using C-miRNA mimic can reverse the key phenotypic features of *miR-146a*-deletion in mice. Noteworthy, we have not observed significant effect of C-miRNA mimic on other immune cell populations in WT mice, such as DCs, B cells or NK cells, even after repeated two-week daily IV injections (Supplemental Fig.S9-10). Finally, our C-miR146a two-week dose-escalation study (5-20mg/kg/day) did not find evidence of toxicities to hematopoietic cells or organ gross abnormalities (Supplemental Fig.S11).

Monocyte-targeted miR146a delivery alleviates cytokine release syndrome triggered by CD19 CAR T-cells without compromising antitumor effects

CAR T-cell immunotherapy has emerged as a revolutionary treatment for various hematologic cancers but many patients experience severe side effects of CRS.[23,33] Recent studies linked CRS to CAR T-cell-dependent activation of CD40 signaling in monocytes/macrophages, thereby inducing IL-1 and IL-6, the key cytokine storm mediators. While CD40 triggers canonical and non-canonical NF-κB signaling, it does not upregulate miR-146a levels.[29] Thus, we tested whether delivery of miR-146a mimic will dampen pro-inflammatory effects of human monocytes induced by the CD19-specific CAR T-cells. Predictably, CD19 CAR T-cells showed low uptake of fluorescently-labeled C-miR146a^{Cy3} compared to monocytes (Supplemental Fig.S12A). C-miR146a did not affect CAR T-cell viability or cytotoxicity against target CD19^{+} Nalm6 leukemia (Figure 5A). Next, we tested C-miR146a in a three-component CRS model co-culturing *in*

vitro: CD19$^+$ Nalm6 cells with CD19-specific CAR T-cells (generated from four different donors' PBMCs) and donor-matched CD14$^+$ monocytes (Figure 5B). The upregulation of IL-1 and IL-6 depended on the presence of monocytes and was induced only by CD19$^+$ leukemia-specific and not mock-transfected CAR T-cells (Figure 5B). Importantly, C-miR146a reduced IL-1 secretion by half, while bringing IL-6 levels close to baseline compared to control treatments. Similar results were obtained using THP-1 monocyte-like cells instead of primary monocytes (Supplemental Fig.S12B-C).

To further confirm that the combination of C-miR146a with CD19 CAR T-cells has potential for alleviating CRS-related toxicities, we adopted a model of CAR T-cell-induced CRS in human CD19$^+$ Raji B-cell lymphoma in partly immunodeficient SCID-Beige mice, similar as recently published.[15] Mice with heavy intraperitoneal lymphoma burden develop CRS and acute inflammation within 3 days after CD19 CAR T-cell injection (Figure 5C). Mice were treated using C-miR146a or control vehicle 3 days before CAR T-cell transfer. As shown in Figure 5DE, the C-miR146a did not interfere with the CAR T-cell mediated inhibition of lymphoma progression. However, the C-miR146a mimic doubled the amount of endogenous miR146a in target peritoneal myeloid cells (Figure 5F). As a result, we observed that C-miR146a dramatically reduced major CRS-related cytokines, IL-6 and G-CSF, likely derived from mouse monocytes in this model as suggested by others (Figure. 5G).[15] Our findings underscore the potential of using C-miR146a mimic to alleviate adverse effects of CD19 CAR T-cell therapy without impeding on-target therapeutic effects.

C-miR146a targets NF-κB signaling and inhibits del(5q) leukemia progression

Low expression of miR-146a located on chromosome 5q has been reported in both MDS and AML since del(5q) aberrations are common in high-risk leukemia.[7] However, constitutive activation of NF-κB survival signaling is not limited to del(5q) MDS/AML and occurs in up to 40% of AML.[34] We tested C-miR-146a mimic effect on viability of HL-60, MDSL del(5q) leukemia cells and also FLT3ITD$^+$/N(5q) MV4-11 AML cells, which all have been found sensitive to small molecule NF-κB inhibitors (Supplemental Fig.S13). As shown in Figure 6A, C-miR146a induced cell death in all three models, although most effectively against miR-146a-deficient MDSL and HL-60 cells. In initial testing, we confirmed that local delivery of C-miR146a into

subcutaneously engrafted leukemia models effectively inhibited growth of both HL-60 (Supplemental Fig.S14A) and MDSL (Supplemental Fig.S14B). Next, we examined the efficacy of systemic C-miR146a administration (10mg/kg) against disseminated HL-60 leukemia. As shown in Figure 6B-D, compared to controls, C-miR146a reduced AML progression and thereby significantly prolonged mice survival. Focused gene expression analysis of a panel of 84 NF-κB-related genes confirmed that C-miR146a downregulated key elements of NF-κB signaling in HL-60 cells, such as *RELA*, *MYD88*, *NFKB1/2, TRAF3, TRAF6* or mediators *IL1B* and *TNF* (Figure 6E and Supplemental Fig.S15). Altogether, these results demonstrate the direct antitumor effect of C-miR146a both *in vitro* and *in vivo*, against miR-146a deficient MDS/AML likely through the inhibition of NF-κB-mediated survival signaling. These conclusions are also supported by analysis of TCGA dataset from 164 AML patients. As expected, low *miR-146a* expression was associated with worse overall patients' survival (Figure 6F). The gene set enrichment analysis (GSEA) indicated significant inverse correlation of miR-146a levels in AML with two different sets of NF-κB-related genes, including *IRAK1*, *NFKB1*, *NFKB2* but not *TRAF6* (Figure 6G-H and Supplemental Fig.S16). Overall, these results underscore therapeutic potential of C-miR146a for treatment of del(5q) MDS/AML and potentially other NF-κB-dependent types of leukemia.

DISCUSSION

In this study, we demonstrate the feasibility of systemic delivery of miRNA mimic specifically to human and mouse myeloid cells for therapeutic modulation of their immune activity or neoplastic growth. The C-miR146a injected intravenously restored miR-146a-5p in target myeloid cells to levels sufficient for complete elimination of exacerbated NF-κB activity in *miR-146a*$^{-/-}$ mice, thereby preventing the exaggerated inflammatory responses and aberrant myeloproliferation. Our miR146a mimic delivery strategy proved effective also in human models of NF-κB-driven inflammation and in myeloid leukemia (MDS/AML). Importantly, unlike standard anti-inflammatory strategies, such as steroid hormones, the myeloid cell-specific miR146a mimic delivery proved effective without interfering with antitumor activity of CAR T-cells or any signs of toxicity even in repeated, long-term administration.

Despite of broad clinical potential, only few miRNA therapeutics entered clinical trials and the majority represented antisense molecules (anti-miRs or antagomirs), which as single-stranded oligonucleotides proved easier to optimize for *in vivo* use.[19,35] One of the best example is targeting lymphoma cell addiction to oncogenic miR-155.[36] In contrast, the therapeutic replacement/restoration of tumor suppressor miRNAs proved challenging. The chemical modification of miRNA to ensure nuclease-resistance can interfere with intracellular processing, RISC loading and/or mRNA targeting. Pharmacologic formulation of miRNA mimics for systemic administration can result in severe immune toxicities.[37] Cell-selective delivery of chemically-stabilized, naked miRNA mimics is gaining attention with a success of siRNA delivery using hepatocyte-specific GalNAc-conjugates[38] and a recent study revisited folate as targeting moiety to miRNA delivery to breast and lung cancer cells.[39]

Our previous studies focused on myeloid cell-selective delivery of oligonucleotides to disrupt immunosuppression in the tumor microenvironment. The conjugation of CpG ODNs with inhibitors of STAT3, a master immune checkpoint regulator, resulted in potent antitumor immune responses. While it seems counterintuitive, the SR/TLR9-mediated delivery strategy can be adapted for dampening excessive immune activity of myeloid cells in autoinflammatory diseases or myeloid malignancies. Unlike type-B CpG sequences, the type-A CpG ODNs are poor activators of NF-κB signaling and cytokines such as IL-6 and IL-10.[40] While recent study showed that injections of CpG(A) alleviated severity of sepsis in mice by

reducing blood clotting,[41] the control CpG(A)-scrRNA did not show anti-inflammatory activity in our experiments. The presence of functional miR-146a-5p guide strand in the CpG conjugate was key to the biological activity of this oligonucleotide. The more extensive chemical modifications of miR-146a guide strand impact its activity, likely interfering with unwinding of the duplex while in RISC.[42] Importantly, even partial restoration of miR-146a-5p levels in target immune cells *in vivo* was sufficient for near complete and durable inhibition of target *IRAK1* and *TRAF6*. The systemic administration of C-miR146a effectively reversed key features of the miR146a-deletion related to excessive NF-κB signaling in both mouse and human myeloid cells. Cytokine storm and CRS occur in response to various conditions from bacterial infections, antibody-based therapies to immunomodulatory drugs. In context of CAR T-cell cancer therapies, especially CD19-specific CAR T-cells, CRS is one of the most common and potentially fatal adverse effects. The lower incidence of CRS correlates with prolonged survival of patients receiving CAR-T therapy.[43] Despite the routine use of the IL-6 receptor antagonist (Tocilizumab), high-dose steroid hormones are frequently required to control severe CRS but at the same time potentially curbing antitumor efficacy of CAR T-cells.[43,44] Hence, the need for more precise and safer immunomodulatory strategies addressing complexity of immune responses. Myeloid cell-selective miR-146a mimic acts at the nodal point of immune cell network, preventing release of cytokines driving CRS from monocytes and macrophages without interfering with CAR T-cell activity.[12,15]

The simplicity and flexibility of the C-miRNA mimic design, adaptable to delivery of both miRNA mimics and anti-miRs, provides as opportunity for the development of miRNA therapeutics for immunomodulation and/or therapy of myeloproliferative diseases and leukemia. The pleiotropic effect of single miRNA on multiple protein targets benefits their potency and reduces development of drug resistance, while the myeloid cell-targeted delivery can improve safety of miRNA therapeutics. The growing list of myeloid cell-specific anti-inflammatory miRNAs extends beyond miR-146a, including recently described miR-125b and miR-203b or tolerance-inducing miR-221 and miR-222.[45,46] In addition to the immunoregulatory role, the miR-146a is well established tumor suppressor and the genetic loss of *miR-146a* or downregulation is common in MDS patients and in AML.[47] MiR-146a replacement using SR/TLR9-targeted delivery provides therapeutic opportunity in MDS/AML patients. However, given the genetic instability of AML, C-miR146a

therapy could likely benefit from combination with targeting additional oncogenic or tumor suppressor miRNAs.[47] The upregulation of oncogenic miR-155 is common in FMS-like tyrosine kinase 3 internal tandem duplication (FLT3-ITD)-associated AML.[48] Noteworthy, miR-155 can potentially antagonize the inhibitory effects of miR-146a on NF-κB in mouse myeloid cells.[20] It is not known whether miR-155 plays similar role lessening tumor suppressive effect of miR-146a in human leukemia but our strategy can be easily adapted to delivery of anti-miR155 to AML cells and leukemia stem cells.[49] Further studies should explore the possibility of personalizing miRNA mimic/antisense combinations to an AML patient-specific miRNA profile using the same SR/TLR9 delivery platform. The emerging CAR T-cell strategies for AML, such as CD123-specific CAR design underscore the potential to combine AML-specific CAR T-cells with C-miR146a, thereby alleviating potential immunotoxicities as well as reducing AML cell survival.[50] We believe that SR/TLR9-targeted delivery of miR-146a mimic provides an outline for development of miRNA therapeutics for a variety of inflammatory disorders and myeloid malignancies.

ACKNOWLEDGEMENTS

The authors would like to thank and acknowledge the dedication of staff members at the DNA/RNA Synthesis, Analytical Cytometry, Light Microscopy Cores and Animal Resources Center (City of Hope).

AUTHORS' CONTRIBUTIONS

Study design: Y.-L.S., M.K.

Data acquisition: Y.-L.S., X.W., M.M., T.A., D.M., Z.Z., D.W., P.S., M.K.

Data analysis and interpretation: Y.-L.S., M.M., T.A., D.M., D.W., C.O.

Administrative, technical, or material support: Y.-L.S., X.W., X.H., B.Z., P.S., S.F., D.B., L.L., G.M., M.B., M.K.

Manuscript writing: Y.-L.S., M.K.

DISCLOSURE OF POTENTIAL CONFLICT OF INTEREST

M.K., P.S., G.M. have a patent on C-miRNA conjugates and uses thereof compositions for the treatment of cancers and other diseases. No potential conflicts of interest were disclosed by the other authors.

GRANT SUPPORT

This work was supported in part by the National Cancer Institute/NIH awards R01CA213131 (to M.K.), Lymphoma SPORE P50CA107399 (to S.F.) and P30CA033572 (to the COH). The content is solely the responsibility of the authors and does not necessarily represent the official views of the NIH.

DATA SHARING

Data have been deposited in GEO, accession number GSE141402

FIGURE LEGENDS

Figure 1. Targeted delivery of miR-146a mimic to RISC/Ago2 complexes in myeloid cells. (A) The design of C-miRNA146a mimic conjugate; underlined: phosphorothioated nucleotides; "o": C3 units of the carbon linker; green: 2'-O-methyl-modified nucleotide. (**B)** Serum stability of miR146a (left) and C-miR146a (right). Oligonucleotides were incubated in 50% human serum at 37°C for the indicated times and then resolved on 7.5M urea/15% PAGE gel. Shown is a representative result from one of three independent experiments; the band intensities were quantified, and the estimated oligonucleotide half-lives were indicated. **(C)** The intracellular uptake of C-miR146a^{Cy3} compared to miR146a^{Cy3} alone by primary human immune cells (monocytes: CD14^{+}; mDCs: CD1c^{+}; pDCs: CD303^{+}; B cells: CD19^{+}; and T cells: CD3^{+}), mouse RAW264.7 macrophages, human MDSL and HL-60 leukemia, human Raji lymphoma and TAIL7 T-cell leukemia cells. Cells were incubated for 1h with 100nM C-miR146a^{Cy3} or miR146a^{Cy3} without any transfection reagents, and the uptake was measured using flow cytometry. **(D)** The intracellular localization of C-miR146a^{Cy3} or miR146a^{Cy3} oligonucleotides (100nM/red) as visualized using confocal microscopy in RAW264.7 cells after 1h incubation. Hoechst33342 (blue) was used for nuclear counterstain. **(E)** The successful loading of miR146a into RISC/Ago2 by C-miRNA conjugate. RAW264.7 or splenocytes isolated from *miR-146a*$^{-/-}$ mice were incubated for 1h with 1μM C-miR146a or miR-146a alone. The RNA-protein complexes were immunoprecipitated using anti-Ago2 or control IgG antibodies and the miR-146a levels were quantified using qPCR. The equal protein loading was confirmed with Western blotting. The data shown represent results from three independent experiments; shown are means±SEM.

Figure 2. C-miR146a mimic targets upstream regulators of NF-κB signaling. (A) C-miR146a inhibits IRAK1 and TRAF6 expression through a sequence-dependent, on-target effect. HEK293T cells were incubated for 24h with 500nM C-miR146a, control C-scrRNA or miR-146a alone, and then transfected with wild-type or mutated *IRAK1* or *TRAF6* 3'UTR-luciferase reporter and control Renilla luciferase plasmids. The reporter luciferase activities were evaluated after 48h. **(B)** Reduced protein levels of IRAK1 and TRAF6 in C-miR146a-treated mouse macrophages and human leukemia cells. IRAK1 and TRAF6 protein levels were assessed using Western blot in RAW264.7 and MDSL cells after 48h incubation with 500nM of

indicated oligonucleotides. Shown are representative results; band intensities were quantified with normalization to β-actin as a loading control. **(C)** MiR146a mimic delivery prevents nuclear translocation of NF-κB. RAW264.7 cells stably expressing p65-eGFP fusion protein were incubated overnight with 500nM C-miR146a or control C-scrRNA and then stimulated with 100ng/mL LPS for 4h. Translocation of NF-κB/p65 (green) into nuclei (blue) was visualized using confocal microscopy; **(D)** C-miR146a inhibits NF-κB DNA binding in target myeloid cells, RAW264.7 or MDSL. Cells were incubated with 500nM C-miR146a, C-anti-miR146a or control C-scrRNA for 48h. The NF-κB DNA binding was assessed in nuclear extracts and verified using p65-specific antibody supershift. Representative blots (left/middle) and the quantification of band intensities combined from three experiments (right). **(E-F)** C-miR146a reduces transcriptional activity of NF-κB in macrophages. RAW-Blue **(E)** or RAW264.7 **(F)** cells were incubated overnight with 500nM C-miR146a or control C-scrRNA and then stimulated with 100ng/mL LPS for 4h. The expression of the NF-κB-dependent reporter gene **(E)** or IL-6 secretion **(F)** were assessed using Quanti-Blue assay or ELISA, respectively. Shown are representative results obtained in three independent experiments; means±SEM.

Figure 3. C-miR146a targets myeloid cell populations and restores miR-146a levels and activity in *miR-146a*$^{-/-}$ mice. (**A, B**) Dose-dependent biodistribution of miR-146a mimic in organs (**A**) and in bone-marrow CD11b^{+} myeloid cells and CD11b^{-} cells (**B**) of *miR-146a*-deficient mice. Mice were injected IV using various doses of C-miR146a and euthanized 3h later to assess miR-146a levels in bone marrow (BM), spleen, lymph nodes (LN), blood, and enriched BM CD11b^{+} myeloid cells and CD11b^{-} cells using qPCR. (**C**) Biodistribution of systemically injected C-miR146a and miR-146a. C57BL/6 mice engrafted with *Cbfb/Myh11/Mpl* leukemia were injected IV with 5 mg/kg C-miR146a^{Cy3} or miR-146a^{Cy3} and euthanized 3h later. The percentages of Cy3^{+} cells in bone marrow were assessed using flow cytometry (T cells: CD3^{+}, NK cells: NK1.1^{+}, B cells: CD19^{+}, ST-HSC: Lin^{-}cKit^{+}Sca1^{+}Flt3^{-}CD150^{-}CD48^{-}, LT-HSC: Lin^{-}cKit^{+}Sca1^{+}Flt3^{-}CD150^{+}CD48^{-}, monocytes: CD11b^{+}CD11c^{-}, macrophages: CD11b^{+}F4/80^{+}, DCs: CD11b^{+}CD11c^{+}, MDSCs: CD11b^{+}Gr1^{+}, and AML cells: GFP^{+}). Shown are results representative for two independent experiments; means ± SEM (*n*=3 mice/group). (**D-E**) Myeloid cell-selective delivery of miR-146a *in vivo*. *miR-146a*$^{-/-}$ or WT mice were injected IV with 5mg/kg C-miR146a and euthanized 3h later. miR-146a levels in BM and

splenocytes and enriched CD11b$^+$ myeloid cells, CD19$^+$ B-cells and CD3$^+$ T-cells from spleen were assessed using qPCR and compared to the same populations in untreated WT mice. Shown are representative results obtained in three independent experiments; means±SEM (*n*=3). (**F**) Single injection of C-miR146a results in transient downregulation of IRAK1 and TRAF6 protein levels. *miR-146a*$^{-/-}$ mice were injected IV with 5 mg/kg C-miR146a and euthanized at indicated times. Protein levels of IRAK1 and TRAF6 in bone marrow cells were assessed using Western blot and the quantified band intensities normalized to β-actin were shown. Shown are results representative for two independent experiments.

Figure 4. C-miR146a corrects the aberrant myeloproliferation and inflammatory responses in *miR146a*-deficient mice. (A-B) Reduced proliferation of *miR-146a*$^{-/-}$ bone marrow-derived macrophages (BMDM) treated with C-miR146a. Bone marrow cells from WT and *miR-146a*$^{-/-}$ mice were cultured in the presence of 50ng/ml M-CSF for 7 days and treated using 1μM C-miR146a or C-scrRNA. The cell proliferation **(A)** was measured using colorimetric XTT assay and the CSF1R expression on CD11b$^+$F4/80$^+$ cells **(B)** was quantified using flow cytometry. **(C-E)** Systemic C-miR146a injections reduced aberrant myeloproliferation of *miR-146a*$^{-/-}$ mice *in vivo*. 10 month old WT or *miR-146a*$^{-/-}$ female mice (*n*=4/group) were injected IV using 10mg/kg C-miR146a or PBS daily for two weeks and euthanized a day after the last injection. Percentages of splenic CD11b$^+$Gr1$^+$ **(C)**, Ki67$^+$CD11b$^+$Gr1$^+$ **(D)**, and the CSF1R expression on macrophages **(E)** were analyzed using flow cytometry. **(F)** Systemic injections of C-miR146a alleviate exaggerated response to endotoxin in *miR-146a*$^{-/-}$ mice. WT or *miR-146a*$^{-/-}$ mice were injected IV with 5mg/kg C-miR146a or C-scrRNA daily for three days before LPS challenge (IP/1mg/kg). Blood was collected at the indicated times to analyze IL-6 and TNF-α levels using ELISA. **(G-J)** C-miR146a treatment restored tolerance to *Listeria monocytogenes* infection in mice with myeloid cell-specific *miR146a*-deletion. WT or *miR-146a*$^{fl/fl}$ mice injected daily IV using 5 mg/kg C-miR146a or C-scrRNA were infected with *L. monocytogenes* on day 3 and euthanized on day 6. The liver bacterial load (**G**), the percentage of weight loss (**H**), plasma levels of IL-6 (**I**) and percentages of various hematopoietic cell populations in circulation (**J**) were assessed. Representative results from at least two independent experiments are shown; means±SEM (*n*=5/group).

Figure 5. Targeting monocytes using C-miR146a mimic alleviates cytokine release syndrome induced by CD19 CAR T-cells without compromising antitumor effects. (A-B) C-miR146a does not affect cytotoxic activity of CD19 CAR T-cells against target leukemia cells. Mock- or CD19 CAR-transduced T cells were co-cultured at a 1:1:1 ratio with donor-matched $CD14^+$ monocytes and target $CD19^+$ Nalm6 B-cell leukemia for 48h in the presence of 500nM C-miR146a or control C-scrRNA. Shown are the percentages of live $CD19^+$ target cells (left) or CAR T-cells (right) vs. untreated control **(A)**. The IL-1 and IL-6 levels in cultured supernatants as measured using ELISA **(B)**. Shown are results combined from four different PBMC donors. **(C)** The experimental design for *in vivo* studies on the CAR T-cell-induced CRS using xenotransplanted lymphoma model. SCID-Beige mice were engrafted with luciferase-expressing Raji lymphoma cells (IP) and after two weeks injected daily using 5mg/kg/IP of C-miR146a or PBS. $12.5x10^6$ mock or CD19 CAR T-cells were injected IP on day 18 before euthanizing mice on day 22. **(D-E)** Tumor progression was monitored using bioluminescent imaging (BLI): ROI, regions of interest; p/s, photons per second; means±SEM. **(F)** The intracellular miR-146a levels were measured using qPCR in $CD11b^+$ myeloid and $CD11b^-$ non-myeloid cells derived from peritoneal lavage. **(G)** Serum human cytokine levels and mouse IL-6 and G-CSF were measured using ELISA after 24h from CAR T-cell transfer. Representative results from at least two independent experiments were shown as means±SEM (*n*=4).

Figure 6. C-miR146a targets NF-κB signaling and inhibits progression of del(5q) MDS and AML. (A) Del(5q) HL-60 or MDSL cells or Flt3 mutation MV4-11 leukemia cells were treated *in vitro* using 500nM C-miR146a or C-scrRNA for 6 days and the percentages of live cells were assessed using flow cytometry. Representative results obtained from three independent experiments; means±SEM. **(B-D)** Systemic administration of C-miR146a extended survival of human HL-60 AML-bearing mice. NSG-SGM3 mice engrafted with disseminated HL-60-luc cells were injected daily IV using 10mg/kg C-miR146a or C-scrRNA and leukemia progression was monitored using BLI **(B),** leukemia progression **(C)** and the Kaplan-Meier survival curves **(D).** Shown are representative results from at least two independent experiments; means±SEM (*n*=10). **(E)** NF-κB pathway gene analysis in HL-60 AML-bearing mice after 10 injections of C-miR146a, C-scrRNA or PBS (*n*=3/group). Total RNA isolated from bone marrow was analyzed using RT^2 Profiler PCR Arrays. The clustergram of significantly (>1.5 fold) downregulated genes. **(F)** Low *miR-146a*

expression is associated with worse overall AML patients' survival based on the TCGA dataset. The optimal cut-point was identified using Log-rank statistics in a survfit model. The log-rank test *P* value is shown. **(G)** Gene Set Enrichment Analysis in AML patients with high versus low miR-146a expression based on TCGA dataset with a NF-κB gene set from Gene Ontology (70 genes). Samples having both miRNA and mRNA expression data (*n*=151) were applied to this analysis. Normalized enrichment score and p-value are shown. **(H)** Standard boxplots were applied to visualize the distribution of $\log_2$-transformed expression of *IRAK1*, *NFKB1*, and *NFkB2* with the low and high miR-146a expression groups. ***$P < 0.001$; **$P < 0.01$.

REFERENCES

1. Mehta A, Baltimore D. MicroRNAs as regulatory elements in immune system logic. *Nat Rev Immunol*. 2016;16(5):279-294.
2. Garzon R, Marcucci G, Croce CM. Targeting microRNAs in cancer: rationale, strategies and challenges. *Nat Rev Drug Discov*. 2010;9(10):775-789.
3. Nejad C, Stunden HJ, Gantier MP. A guide to miRNAs in inflammation and innate immune responses. *FEBS J*. 2018;285(20):3695-3716.
4. Kasinski AL, Slack FJ. Epigenetics and genetics. MicroRNAs en route to the clinic: progress in validating and targeting microRNAs for cancer therapy. *Nat Rev Cancer*. 2011;11(12):849-864.
5. Nicoloso MS, Spizzo R, Shimizu M, Rossi S, Calin GA. MicroRNAs--the micro steering wheel of tumour metastases. *Nat Rev Cancer*. 2009;9(4):293-302.
6. Wallace JA, O'Connell RM. MicroRNAs and acute myeloid leukemia: therapeutic implications and emerging concepts. *Blood*. 2017;130(11):1290.
7. Starczynowski DT, Morin R, McPherson A, et al. Genome-wide identification of human microRNAs located in leukemia-associated genomic alterations. *Blood*. 2011;117(2):595-607.
8. Starczynowski DT, Kuchenbauer F, Argiropoulos B, et al. Identification of miR-145 and miR-146a as mediators of the 5q- syndrome phenotype. *Nat Med*. 2010;16(1):49-58.
9. Boldin MP, Taganov KD, Rao DS, et al. miR-146a is a significant brake on autoimmunity, myeloproliferation, and cancer in mice. *J Exp Med*. 2011;208(6):1189-1201.
10. Zhao JL, Rao DS, Boldin MP, Taganov KD, O'Connell RM, Baltimore D. NF-kappaB dysregulation in microRNA-146a-deficient mice drives the development of myeloid malignancies. *Proc Natl Acad Sci U S A*. 2011;108(22):9184-9189.
11. Boldin MP, Baltimore D. MicroRNAs, new effectors and regulators of NF-kappaB. *Immunol Rev*. 2012;246(1):205-220.
12. Norelli M, Camisa B, Barbiera G, et al. Monocyte-derived IL-1 and IL-6 are differentially required for cytokine-release syndrome and neurotoxicity due to CAR T cells. *Nat Med*. 2018;24(6):739-748.
13. Halkein J, Tabruyn SP, Ricke-Hoch M, et al. MicroRNA-146a is a therapeutic target and biomarker for peripartum cardiomyopathy. *J Clin Invest*. 2013;123(5):2143-2154.
14. O'Connell RM, Rao DS, Baltimore D. microRNA regulation of inflammatory responses. *Annu Rev Immunol*. 2012;30:295-312.
15. Giavridis T, van der Stegen SJC, Eyquem J, Hamieh M, Piersigilli A, Sadelain M. CAR T cell-induced cytokine release syndrome is mediated by macrophages and abated by IL-1 blockade. *Nat Med*. 2018;24(6):731-738.
16. Lieberman J. Tapping the RNA world for therapeutics. *Nat Struct Mol Biol*. 2018;25(5):357-364.
17. Ling H, Fabbri M, Calin GA. MicroRNAs and other non-coding RNAs as targets for anticancer drug development. *Nature Reviews Drug Discovery*. 2013;12:847.
18. Chen Y, Gao DY, Huang L. In vivo delivery of miRNAs for cancer therapy: challenges and strategies. *Adv Drug Deliv Rev*. 2015;81:128-141.
19. Rupaimoole R, Slack FJ. MicroRNA therapeutics: towards a new era for the management of cancer and other diseases. *Nat Rev Drug Discov*. 2017;16(3):203-222.
20. Mann M, Mehta A, Zhao JL, et al. An NF-kappaB-microRNA regulatory network tunes macrophage inflammatory responses. *Nat Commun*. 2017;8(1):851.
21. Kortylewski M, Swiderski P, Herrmann A, et al. In vivo delivery of siRNA to immune cells by conjugation to a TLR9 agonist enhances antitumor immune responses. *Nat Biotechnol*. 2009;27(10):925-932.
22. Zhang Q, Hossain DM, Duttagupta P, et al. Serum-resistant CpG-STAT3 decoy for targeting survival and immune checkpoint signaling in acute myeloid leukemia. *Blood*. 2016;127(13):1687-1700.
23. Wang X, Popplewell LL, Wagner JR, et al. Phase 1 studies of central memory-derived CD19 CAR T-cell therapy following autologous HSCT in patients with B-cell NHL. *Blood*. 2016;127(24):2980-2990.
24. Alizadeh D, Wong RA, Yang X, et al. IL15 Enhances CAR-T Cell Antitumor Activity by Reducing mTORC1 Activity and Preserving Their Stem Cell Memory Phenotype. *Cancer Immunol Res*. 2019;7(5):759-772.
25. Verthelyi D, Ishii KJ, Gursel M, Takeshita F, Klinman DM. Human peripheral blood cells differentially recognize and respond to two distinct CPG motifs. *J Immunol*. 2001;166(4):2372-2377.

26. Zhang Q, Hossain DM, Nechaev S, et al. TLR9-mediated siRNA delivery for targeting of normal and malignant human hematopoietic cells in vivo. *Blood*. 2013;121(8):1304-1315.
27. Sakai J, Cammarota E, Wright JA, et al. Lipopolysaccharide-induced NF-kappaB nuclear translocation is primarily dependent on MyD88, but TNFalpha expression requires TRIF and MyD88. *Sci Rep*. 2017;7(1):1428.
28. Su YL, Swiderski P, Marcucci G, Kortylewski M. Targeted Delivery of miRNA Antagonists to Myeloid Cells In Vitro and In Vivo. *Methods Mol Biol*. 2019;1974:141-150.
29. Taganov KD, Boldin MP, Baltimore D. MicroRNAs and immunity: tiny players in a big field. *Immunity*. 2007;26(2):133-137.
30. Magilnick N, Reyes EY, Wang WL, et al. miR-146a-Traf6 regulatory axis controls autoimmunity and myelopoiesis, but is dispensable for hematopoietic stem cell homeostasis and tumor suppression. *Proc Natl Acad Sci U S A*. 2017;114(34):E7140-E7149.
31. Lucke K, Yan I, Krohn S, et al. Control of Listeria monocytogenes infection requires classical IL-6 signaling in myeloid cells. *PLoS One*. 2018;13(8):e0203395.
32. Cho S, Lee HM, Yu IS, et al. Differential cell-intrinsic regulations of germinal center B and T cells by miR-146a and miR-146b. *Nat Commun*. 2018;9(1):2757.
33. Sterner RM, Sakemura R, Cox MJ, et al. GM-CSF inhibition reduces cytokine release syndrome and neuroinflammation but enhances CAR-T cell function in xenografts. *Blood*. 2018.
34. Zhou J, Ching YQ, Chng WJ. Aberrant nuclear factor-kappa B activity in acute myeloid leukemia: from molecular pathogenesis to therapeutic target. *Oncotarget*. 2015;6(8):5490-5500.
35. Setten RL, Rossi JJ, Han SP. The current state and future directions of RNAi-based therapeutics. *Nat Rev Drug Discov*. 2019.
36. Cheng CJ, Bahal R, Babar IA, et al. MicroRNA silencing for cancer therapy targeted to the tumour microenvironment. *Nature*. 2015;518(7537):107-110.
37. Beg MS, Brenner AJ, Sachdev J, et al. Phase I study of MRX34, a liposomal miR-34a mimic, administered twice weekly in patients with advanced solid tumors. *Invest New Drugs*. 2017;35(2):180-188.
38. Springer AD, Dowdy SF. GalNAc-siRNA Conjugates: Leading the Way for Delivery of RNAi Therapeutics. *Nucleic Acid Ther*. 2018;28(3):109-118.
39. Orellana EA, Tenneti S, Rangasamy L, Lyle LT, Low PS, Kasinski AL. FolamiRs: Ligand-targeted, vehicle-free delivery of microRNAs for the treatment of cancer. *Sci Transl Med*. 2017;9(401).
40. Vollmer J, Krieg AM. Immunotherapeutic applications of CpG oligodeoxynucleotide TLR9 agonists. *Adv Drug Deliv Rev*. 2009;61(3):195-204.
41. Yamamoto Y, Sugimura R, Watanabe T, et al. Class A CpG Oligonucleotide Priming Rescues Mice from Septic Shock via Activation of Platelet-Activating Factor Acetylhydrolase. *Front Immunol*. 2017;8:1049.
42. Adams BD, Parsons C, Walker L, Zhang WC, Slack FJ. Targeting noncoding RNAs in disease. *J Clin Invest*. 2017;127(3):761-771.
43. Neelapu SS, Tummala S, Kebriaei P, et al. Chimeric antigen receptor T-cell therapy - assessment and management of toxicities. *Nat Rev Clin Oncol*. 2018;15(1):47-62.
44. Park JH, Riviere I, Gonen M, et al. Long-Term Follow-up of CD19 CAR Therapy in Acute Lymphoblastic Leukemia. *N Engl J Med*. 2018;378(5):449-459.
45. Sisti F, Wang S, Brandt SL, et al. Nuclear PTEN enhances the maturation of a microRNA regulon to limit MyD88-dependent susceptibility to sepsis. *Sci Signal*. 2018;11(528).
46. Seeley JJ, Baker RG, Mohamed G, et al. Induction of innate immune memory via microRNA targeting of chromatin remodelling factors. *Nature*. 2018;559(7712):114-119.
47. Wallace JA, O'Connell RM. MicroRNAs and acute myeloid leukemia: therapeutic implications and emerging concepts. *Blood*. 2017;130(11):1290-1301.
48. Gerloff D, Grundler R, Wurm AA, et al. NF-kappaB/STAT5/miR-155 network targets PU.1 in FLT3-ITD-driven acute myeloid leukemia. *Leukemia*. 2015;29(3):535-547.
49. Zhang B, Nguyen LXT, Li L, et al. Bone marrow niche trafficking of miR-126 controls the self-renewal of leukemia stem cells in chronic myelogenous leukemia. *Nat Med*. 2018;24(4):450-462.
50. Mardiros A, Dos Santos C, McDonald T, et al. T cells expressing CD123-specific chimeric antigen receptors exhibit specific cytolytic effector functions and antitumor effects against human acute myeloid leukemia. *Blood*. 2013;122(18):3138-3148.

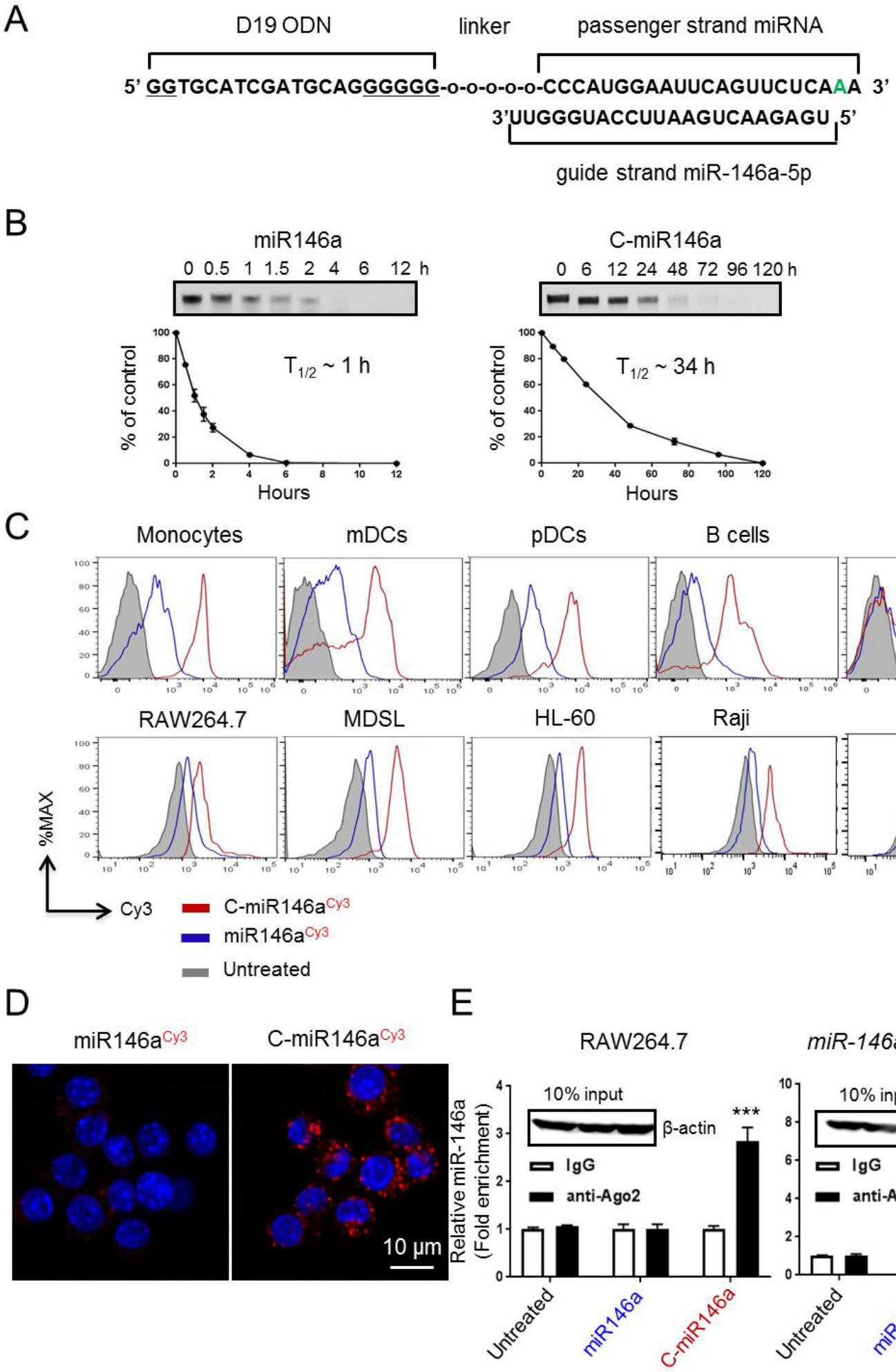

Figure. 1

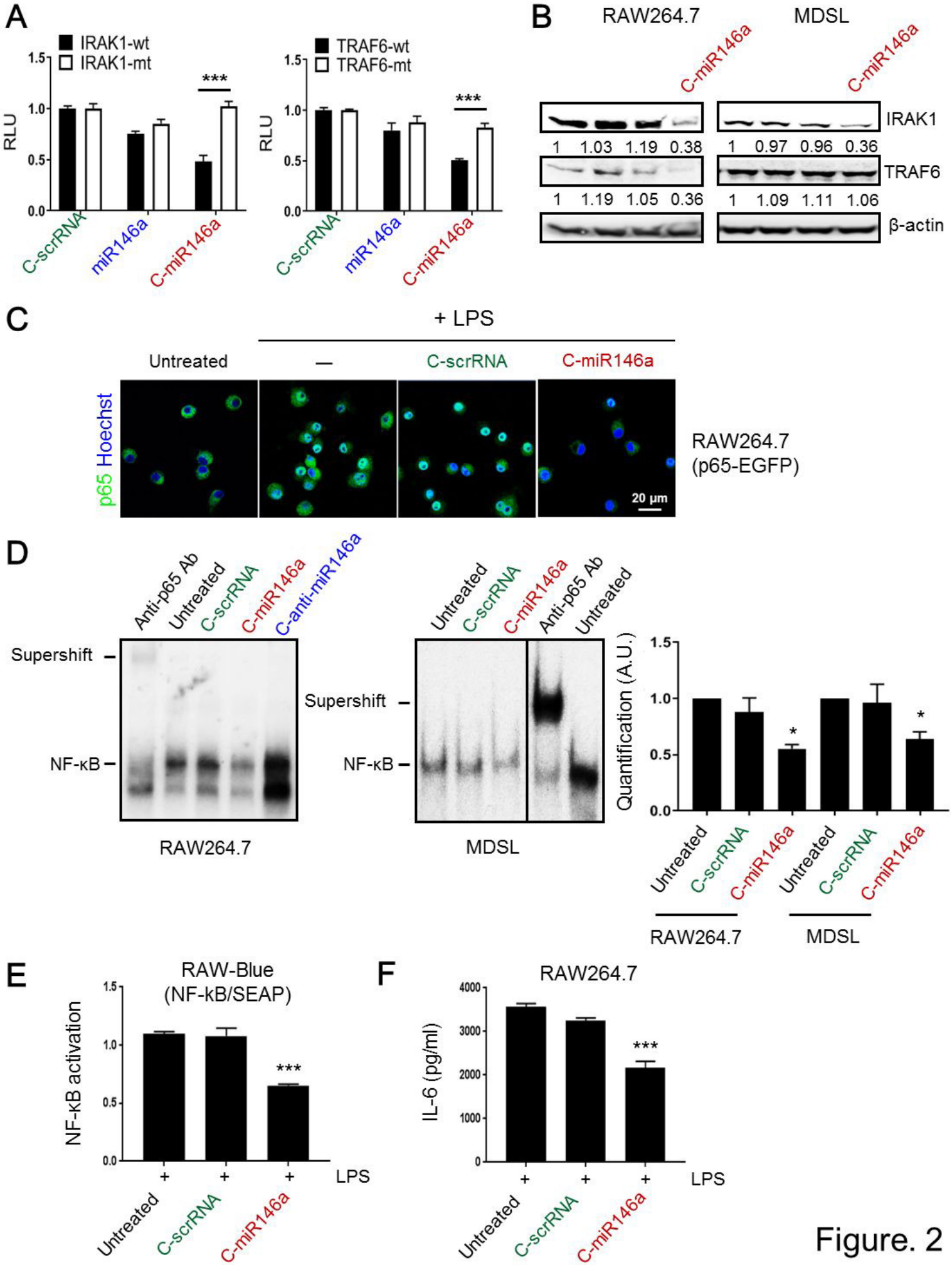

Figure. 2

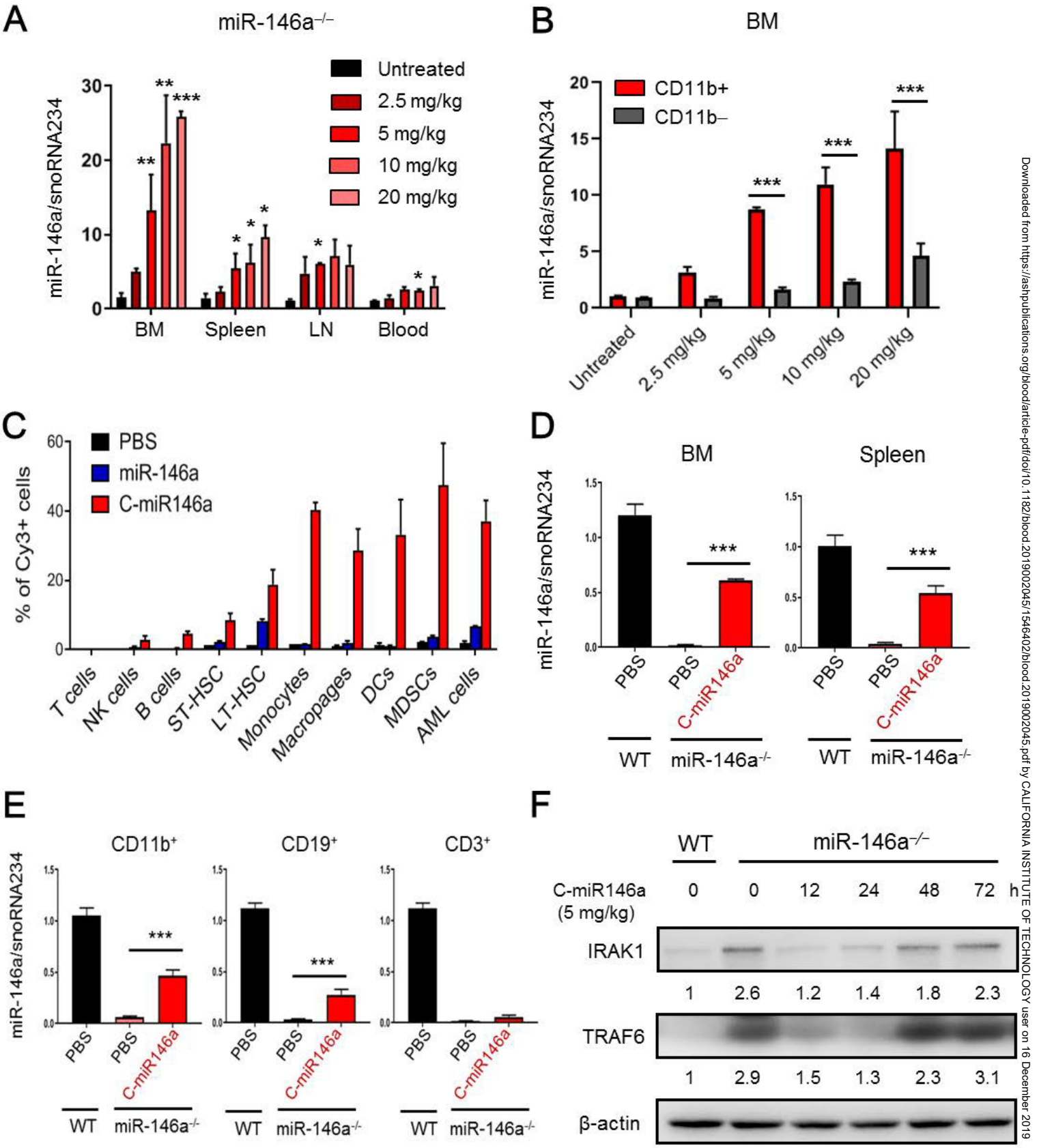

Figure. 3

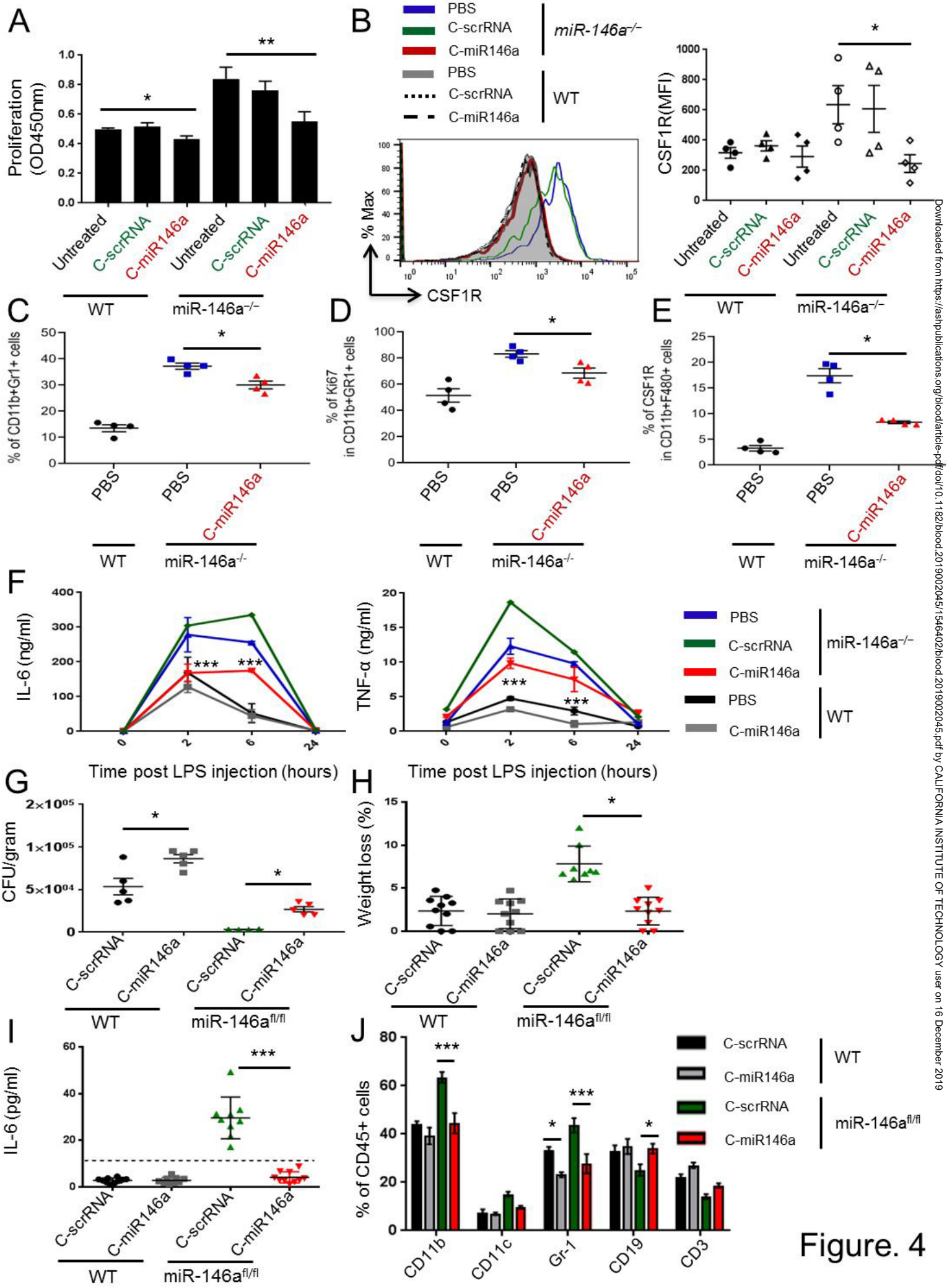

Figure. 4

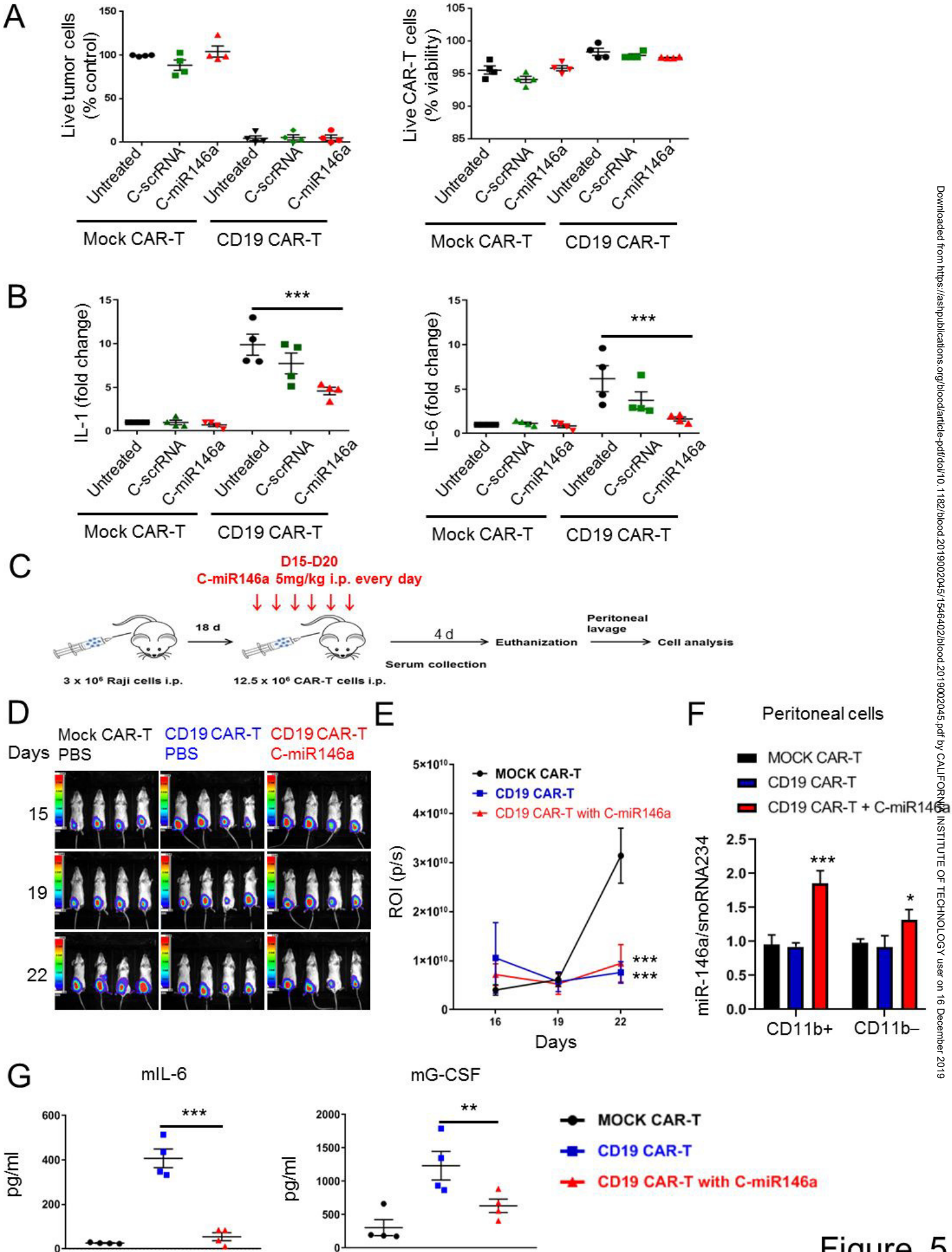

Figure. 5

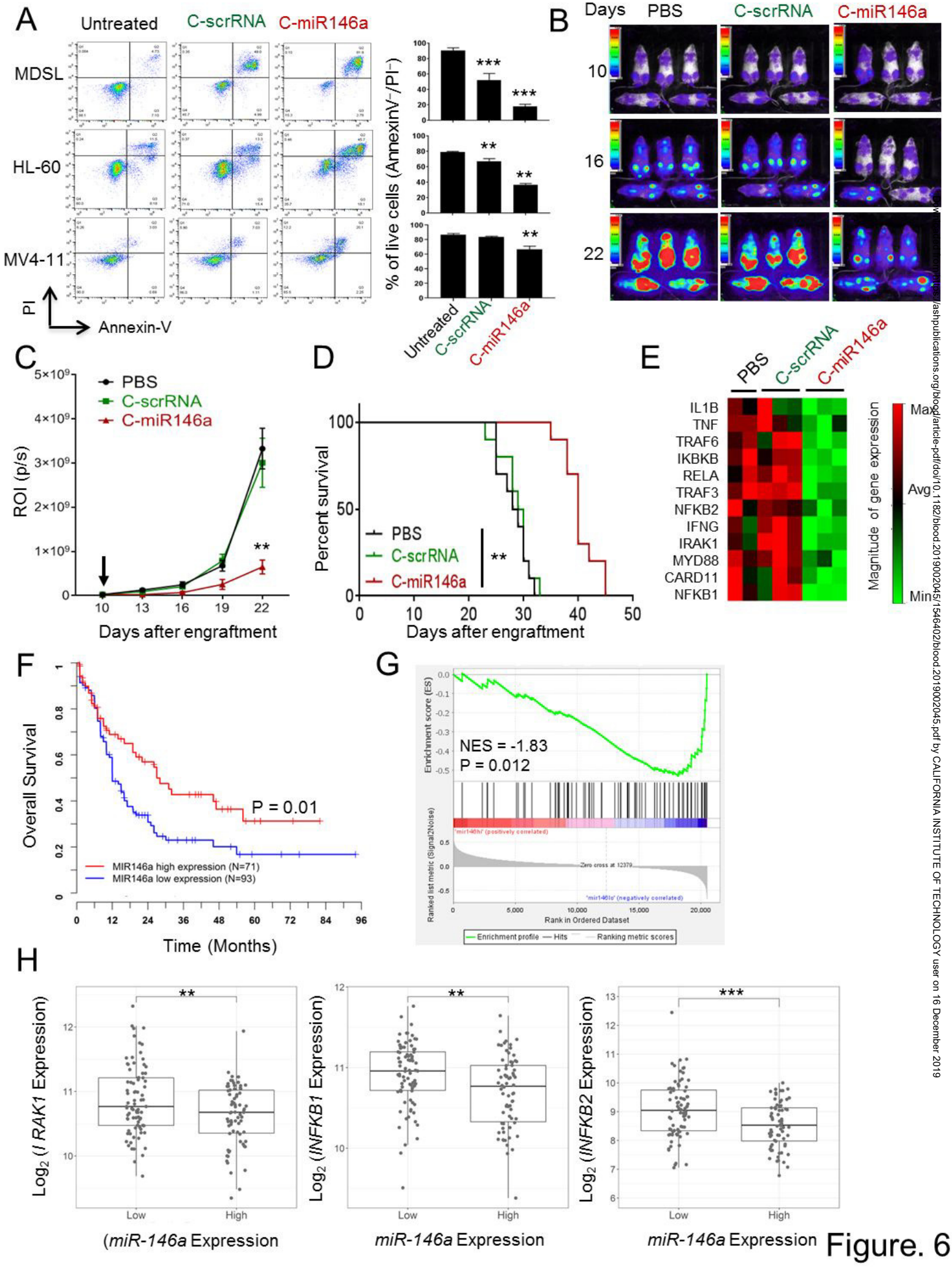

Figure. 6